JTTEE5 14:77-84
DOI: 10.1361/10599630522747

High-Velocity Oxyfuel Reactive Spraying of Mechanically Alloyed Ni-Ti-C Powders

A.J. Horlock, Z. Sadeghian, D.G. McCartney, and P.H. Shipway

(Submitted September 3, 2003; in revised form March 5, 2004)

Recently, there has been considerable interest in producing cermet coatings with nanoscale carbide grains in the size range 50 to 500 nm. In this article, the production of nanoscale TiC grains in a Ni-based alloy matrix by reactive high-velocity oxyfuel (HVOF) spraying of metastable Ni-Ti-C powder is reported. Mechanical alloying of a Ni(Cr) prealloyed powder and Ti and C elemental powders was performed in a planar-type ball mill, and materials were characterized in detail using x-ray diffraction (XRD) and scanning electron microscopy (SEM). Phase changes were correlated with milling time and other processing conditions. Results show that, by the selection of appropriate conditions, a metastable Ni-Ti-C powder could be obtained with the nominal composition 50wt.%Ni-40wt.%Ti-10wt.%C. Following sieving and classification, powder was produced with a particle size range of −38 to 8 μm, which is suitable for HVOF spraying. Coatings, approximately 250 μm thick, were deposited by HVOF spraying onto mild steel substrates, and the microstructures formed were investigated. XRD showed that a self-propagating high-temperature synthesis (SHS) reaction had occurred in the powder particles during spraying and that the principal phases present in the coating were TiC and a Ni-rich solid solution; small quantities of NiTi, TiO_2, and $NiTiO_3$ were also present. SEM revealed that the coatings had a characteristic, splatlike morphology and that TiC formed as a nanoscale dispersion, with a size range of ~50 to 200 nm, within solidified splats. The microstructures of these reactively sprayed Ni-TiC coatings are briefly compared with those observed in HVOF-sprayed coatings deposited using prereacted SHS powder.

Keywords high-velocity oxyfuel spraying, microstructure, nanostructured coating, self-propagating high-temperature synthesis, TiC

1. Introduction

In recent years, there has been significant interest in the production of TiC-based cermet coatings by high-velocity oxyfuel (HVOF) spraying for applications in which resistance to wear and oxidation or corrosion is required (Ref 1-5). Normally, TiC is produced by high-temperature processes such as the displacement reaction between TiO_2 and C, or the direct reaction of elemental Ti and C, both of which require expensive furnaces. The self-propagating high-temperature synthesis (SHS) of TiC from elemental Ti and C powders is an attractive, alternative route that can be used due to the large negative enthalpy of formation of TiC. Self-propagating high-temperature synthesis is a combustion process in which an exothermic, self-sustaining chemical reaction propagates through a premixed powder compact in the form of a high-temperature reaction front (Ref 6). With this process, it is possible to make additions of metallic diluents, such as Ni and Cr, which do not take part in the synthesis reaction. They form an alloyed, metallic binder phase for the TiC, and this possesses specific properties, for example, ductility, good corrosion, and oxidation resistance. A factor that limits the maximum amount of such additions is the heat that Ni and Cr absorb during the SHS reaction. Bartuli et al. (Ref 7) have reviewed the production of SHS powders for thermal spray applications, and it was found that in the Ni(Cr)-TiC system cermet powders with TiC contents as low as 40 wt.% can be formed. The production of powder and HVOF-sprayed coatings based on a 35wt.%Ni(Cr)-65wt.%TiC composition has been reported previously (Ref 5). This involved the manufacture of SHS-reacted compacts that were then crushed, ground, and classified to a particle size range suitable for HVOF spraying. However, the yields of powder in a size range suitable for thermal spraying were generally not high (Ref 4, 5). Moreover, it was not possible to decrease the TiC grain size below about 5 μm, which prevented an investigation into the properties of coatings with nanoscale TiC grains. An alternative method for the production of nanoscale TiC is to use mechanical alloying (MA) before the initiation of the SHS reaction, as described by Wu et al. (Ref 8). A modified form of this is the basis of the current study in which a powder having a nominal composition of 50wt.%Ni(Cr)-40wt.%Ti-10wt.%C is produced by MA, with conditions selected so that Ti and C are retained within a Ni(Cr) matrix in an unreacted (i.e., a metastable) state. The SHS reaction to produce TiC is then initiated within individual powder particles during HVOF spraying by the heat input from the combustion gases, leading to the formation of a coating containing TiC particles within a Ni-rich matrix (i.e., a cermet). A prealloyed Ni(Cr) powder was used to produce a metallic matrix with the potential to resist corrosion and high-temperature oxidation, while TiC is a ceramic with

The original version of this paper was published as part of the ASM Proceedings, *Thermal Spray 2003: Advancing the Science and Applying the Technology*, International Thermal Spray Conference (Orlando, FL), May 5-8, 2003, Basil R. Marple and Christian Moreau, Ed., ASM International, 2003.

A.J. Horlock, Z. Sadeghian, D.G. McCartney, and **P.H. Shipway,** School of Mechanical, Materials, Manufacturing Engineering and Management, University of Nottingham, Nottingham, NG7 2RD, United Kingdom. Contact e-mail: graham.mccartney@nottingham.ac.uk.

high hardness and chemical stability. This reactive spraying principle has been demonstrated previously using Al-Cr_2O_3 (Ref 9) and Fe-Ti-B (Ref 10) mixtures to generate an SHS reaction during plasma spraying, but, to date, this approach does not appear to have been investigated for the production of cermet coatings by HVOF spraying.

Mechanical alloying is a powder metallurgical process that provides a solid-state route for producing intimately mixed, fine-scale composite powders from elemental and master alloy starting powders. It involves a complex process of deformation, fragmentation, cold welding, and microdiffusion, occurring within a thin layer of powder trapped between two colliding surfaces during impact (Ref 11, 12). In the present work, a planar-type ball mill was used that consists of ferromagnetic hardened steel balls confined in a stainless steel chamber. The ball movement during the milling process is confined to the vertical plane by the chamber walls, and the milling energy is controlled by changing the position of external, high-field, permanent magnets (Ref 12-14).

In the HVOF process (Ref 15), powder particles, typically in the size range 15 to 63 μm, are injected into a high-velocity hot gas jet generated by the combustion of oxygen with a fuel such as hydrogen or propylene. The powder particles are heated and accelerated toward the substrate to be coated with a heating time on the order of 1 to 3 ms. Just prior to impact with the substrate, they will be in a molten or semimolten, softened state, depending on the process conditions used. On impact with the substrate, the particles cool and solidify rapidly, and a thick coating (250-500 μm) is normally built up by scanning the spray gun across the substrate in a number of passes. It is evident therefore that, providing a particle contains an appropriate quantity of the necessary constituent elements, the opportunity exists to initiate an SHS reaction within each particle. As a result of the rapid heat input to individual powder particles and the short residence time in the molten state there is thus the potential to produce a coating with fine-scale TiC dispersed in a metallic matrix.

This article describes investigations into the following: the planar-type ball milling of Ni(Cr), Ti, and C powders to form a metastable, mechanically alloyed powder; the HVOF spraying of the resultant powder; and the microstructural characterization of powders and coatings.

2. Experimental

2.1 Materials

The constituent powder materials used for this investigation were Ni(Cr), Ti, and C. The Ni(Cr) was a prealloyed powder of composition 80wt.%Ni-20wt.%Cr (catalog reference NI-105-2) supplied by Praxair Thermal Spray Products (Indianapolis, IN). The Ti, of commercial purity (99.7%), and C were supplied by London & Scandinavian Metallurgical Company (Rotherham, UK). The Ni(Cr) powder was produced by inert gas atomization and had a near spherical morphology with a nominal particle size range 15 to 45 μm. The Ti was derived from sponge material, was angular in shape, and was supplied in the size range 100 to 500 μm. The C was nondusting, granular in form, with a nominal particle size of approximately 1 μm.

Table 1 HVOF spray parameters

Spray parameter	Units	Value
Total gas flow	N 1 min^{-1}	856
Oxygen flow	N 1 min^{-1}	212
Hydrogen flow	N 1 min^{-1}	623
Nitrogen flow	N 1 min^{-1}	21
O_2-to-fuel gas ratio	% of stoichiometry	68

2.2 Powder Processing and HVOF Spraying

The constituent materials were milled using a planar-type Uni-Ball Mill II (Australian Scientific Instruments, a Division of Anutech Pty. Ltd., Canberra, Australia) with a stainless steel chamber (inner diameter 200 mm; depth 28 mm) containing 12 ferromagnetic steel balls of 25 mm diameter. A fixed rotational speed of 100 rpm was used throughout the experiments. Before the commencement of milling, the chamber was evacuated and backfilled with nitrogen to obtain a controlled atmosphere, thus minimizing the potential for the oxidation of the Ti powder and the Ti fines produced during milling.

In initial experiments, the constituent powders, Ni(Cr), Ti, and C, were mixed in the mass ratio 50 to 40 to 10, were placed in the chamber of the mill, and were milled for times ranging from 72 to 100 h. However, on opening the chamber and exposing the milled product to air, a spontaneous SHS reaction between the Ti and C occurred. To avoid this, and to obtain a metastable product, a three-step process was developed. First, the Ni(Cr) and Ti powders were milled together in the mass ratio 1 to 1. Then the Ni(Cr) and C powders were also milled in the ratio 1 to 1. Finally, both milled products were mixed in the mass ratio 4 to 1 and were milled together as the final step in the process. The powder required for thermal spraying, with a nominal size range of +8 −38 μm, was obtained by mechanically sieving the final MA metastable product using a 38 μm screen on an Octagon Digital Sieve Shaker (Endecotts Ltd., London, UK) followed by air classification to remove <10 μm fines. Experiments were carried out to investigate the effects of (a) milling time and (b) quantities of powder constituents on the phases formed during milling, the development of powder microstructure, and the yield of sprayable metastable powder.

The coatings were produced with a UTP Top Gun/Miller HVOF thermal spray system (Praxair Surface Technologies, Appleton, WI) using a 22 mm long combustion chamber. Grit-blasted mild steel coupons (50 × 25 × 2 mm) were used as substrates onto which the coatings were deposited. These were mounted on a turntable with a vertical axis of rotation (surface rotational speed ~1 ms^{-1}) with the HVOF gun being traversed vertically at 5 mms^{-1} with a standoff distance of 200 mm. Air jets were used to cool the substrates during deposition, and 34 gun passes were used to deposit the coating to a thickness of ~250 μm. The spray parameters, summarized in Table 1, were selected to minimize the oxidation of the powder and to achieve a low-porosity deposit. Further details of the experimental setup have been described previously elsewhere (Ref 4, 5).

2.3 Materials Characterization

The materials were characterized by microstructural analysis, phase identification, and powder particle size distribution.

Investigation of the powder morphology and the cross-sectional microstructures of the powder and the coatings were performed using a Jeol 6400 scanning electron microscope (SEM) (JEOL (UK) Ltd., Welwyn Garden City, UK) using secondary electron and backscattered electron (BSE) imaging and energy-dispersive x-ray (EDX) analysis. The morphology of the powder was observed by mounting it on an adhesive carbon disc and sputter gold coating. The cross sections through the powder particles and coatings were obtained by mounting in conducting resin and by using conventional preparation techniques of grinding and polishing to a 1 μm finish. High-resolution SEM images of the coating were obtained using a Philips XL30 ESEM with a field emission gun (FEI Ltd., Cambridge, UK). Phases were identified by x-ray diffraction (XRD) using a Siemens D500 diffractometer (Siemens Analytical X-Ray Instruments, Sunbury-on-Thames, UK) employing monochromatic CuKα radiation (λ = 0.15404 nm). The XRD scans were performed with a step size of 0.05° and a dwell time per step of 2 s. Powder particle size distributions were determined by laser diffractometry using a Malvern Mastersizer S (Malvern Instruments Ltd., Worcestershire, UK).

3. Results

The results are reported in four sections: (1) the development of the Ni(Cr)-Ti mechanically alloyed powder, (2) the development of the Ni(Cr)-C powder, (3) the milling together of the products of (1) + (2), and (4) the HVOF-sprayed coating obtained from the sieved and classified metastable MA powder.

3.1 Ni(Cr)-Ti Powder

Figure 1(a) shows a typical microstructure of the powder produced by milling 50 g of Ni(Cr) and 50 g of Ti powder together for 72 h. The micrograph shows areas of bright and dark contrast. The bright regions were determined, by EDX analysis, to be a Ni-rich phase, and areas of darker contrast were determined to be a Ti-rich phase. Increasing the milling time resulted in a more pronounced lamellar or layered morphology of Ni-rich and Ti-rich phases, which is typical of MA. Figure 1(b) shows a typical structure following 100 h of milling. The particle size analysis of the premilled and postmilled powder shows an increase in average particle size following milling, as shown in Fig. 2. The powder appeared to go through a transition, observed in the 72 h milled sample, with a small number of large particles that were >200 μm when formed. This was confirmed by SEM observation. However, after 100 h of milling the proportion of these large particles decreased significantly. The XRD patterns of the powder after different milling times are shown in Fig. 3. It can be observed that both the face-centered cubic (fcc) Ni peaks, at 2θ values of ~44° and 52°, and close-packed hexagonal (cph) Ti peaks, at 2θ values of 35°, 38°, and 40°, were broadened (and decreased in intensity) with increasing time of milling, but no new phases were formed. The peak broadening can be caused by a number of factors such as an increase in the dislocation density and a decrease of the grain size in the phases present in the powder.

3.2 Ni(Cr)-C Powder

The progression of the MA process for 50 g of Ni(Cr) and 50 g of C was more difficult to monitor, and intimate layered structures were generally not observed, even after 100 h of milling. Figure 4 shows a particle of Ni(Cr) that had particles of C embedded within it. However, the proportion of the powder showing this structure was low. Figure 5, which shows plots of particle size distribution before and after milling, does indicate that the proportion of small C particles in the size range 1 to 10 μm was considerably reduced compared with the as-mixed distribution. The volume percent of particles in the size range 15 to 45 μm (the size of the original Ni(Cr) particles) had increased after milling. Overall, this suggests that some C became incorporated into the metallic particles, possibly as a solid solution in addition to being entrained as elemental C. A significant quantity of large granular clumps of C (>100 μm) seemed to be retained even after milling, and this, along with the particles <10 μm in size, indicated that a considerable amount of free C was still present after milling. The XRD patterns of the Ni(Cr)-plus-C powder in the as-mixed condition and after 100 h of milling are shown in Fig. 6. High-intensity peaks corresponding to crystalline fcc Ni solid

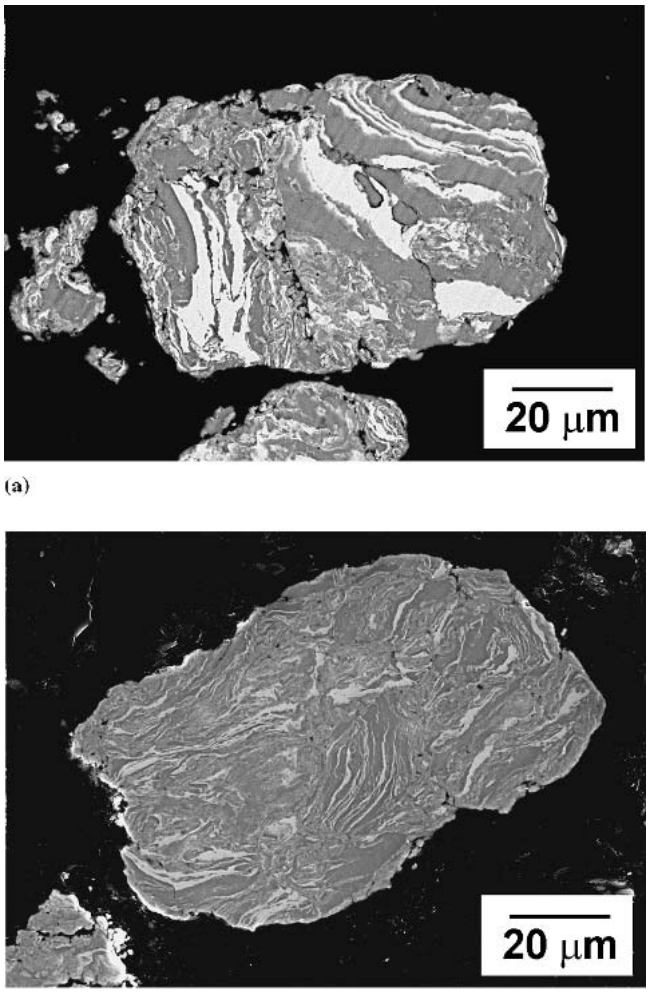

Fig. 1 (a) BSE image of a section through a powder particle following 72 h of milling of Ti and Ni(Cr) powders. A layered microstructure is revealed comprising Ti-rich (dark) and Ni(Cr)-rich (light) phases. (b) BSE image as in (a) but following 100 h of milling, showing layers of reduced thickness

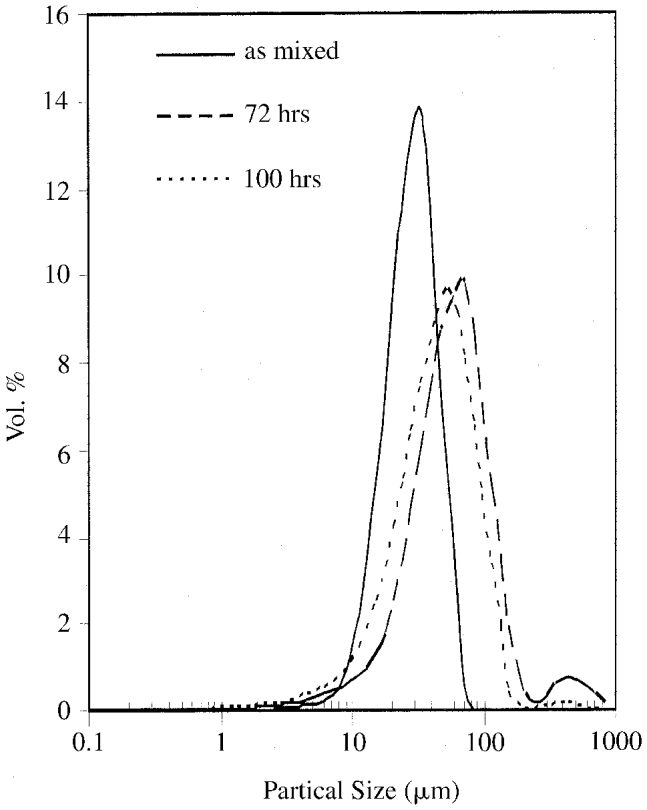

Fig. 2 Graph showing particle size distribution plots obtained from laser diffractometer measurements on powder samples in the following conditions, as shown in the legend: as-mixed Ni(Cr) and Ti powders, Ni(Cr) and Ti powders following milling for 72 h, and after milling the powders for 100 h

solution are evident both before and after milling. There is a broad peak arising from the carbon at 2θ values of ~25° in the as-mixed powder. After milling had taken place, this peak was seen to have broadened and decreased in intensity, presumably due to several factors such as C dissolution in Ni and also amorphization of the C during milling, a feature that has been noted previously (Ref 8).

3.3 Ni(Cr)Ti + Ni(Cr)C Powder

Figure 7 shows a powder particle after milling 80 g of Ni(Cr)-Ti with 20 g of Ni(Cr)-C for 100 h (i.e., the product of 1 and 2 in the ratio of 4 to 1). This shows the banded structure of Ni(Cr) (light phase) and Ti (gray phase) with some dark contrast areas, which indicate the presence of free C. To determine whether this milled product was capable of an SHS reaction, a 12 mm diameter × 12 mm long compact was pressed in a uniaxial die and placed in a furnace at 900 °C. An SHS reaction was observed as the temperature of the compact was raised. Figure 8 shows XRD patterns obtained from powder following milling and from a sample of the reacted compact following furnace treatment. For the milled powder, there are peaks associated with Ni and Ti solid solutions, but there was no evidence for the presence of TiC. However, the XRD pattern from the furnace-heated sample showed strong TiC peaks at 2θ values of 36.5° and 42°, confirming that an SHS reaction had occurred. Particle size analysis re-

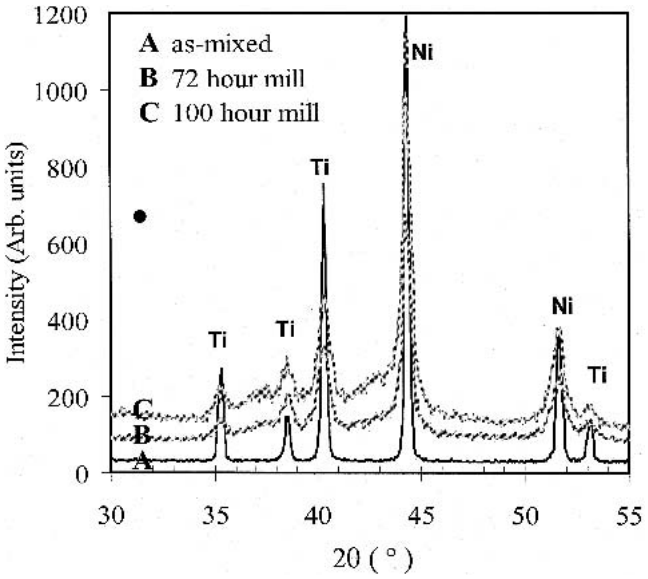

Fig. 3 The XRD patterns obtained from Ni(Cr) + Ti powder samples in the following conditions: (A) as-mixed, (B) following milling for 72 h, and (C) after milling for 100 h. Peaks corresponding to the crystalline structures of fcc Ni and cph Ti are present in all three patterns.

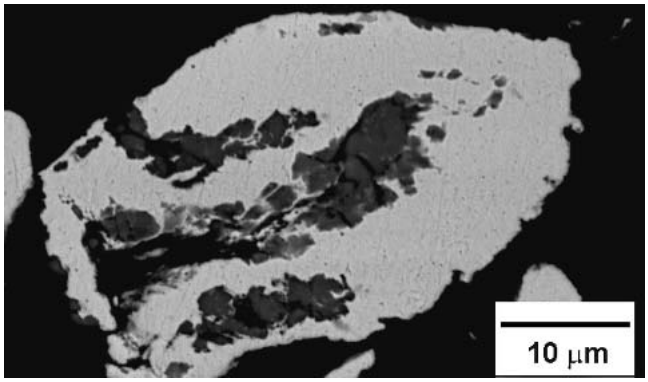

Fig. 4 A BSE image of a section through a powder particle following 100 h of milling of C and Ni(Cr) powders. Carbon-rich regions (dark) are embedded within a Ni-rich matrix (light).

vealed that the accumulated powder from a number of milled batches of Ni(Cr)Ti + Ni(Cr)C was bimodal in character (Fig. 9) and contained significant amounts of powder particles of <5 μm, which could not be used in HVOF spraying. The MA powder was sieved and air-classified, as described in Section 2.2, and the size distributions of the resultant fractions are also plotted in Fig. 9. The external morphology of the powder, which was used as feedstock in the HVOF-spraying experiments, is shown in Fig. 10.

3.4 HVOF Sprayed Coating

Figure 11(a) and (b) show BSE images of the cross section through a coating. As seen in Fig. 11(a), the distribution of the phases is relatively uniform throughout the coating. There is little evidence of porosity, and the coating appears well-bonded to the steel substrate. The splatlike, layered morphology was found to comprise Ni-rich splats, splats containing appreciable

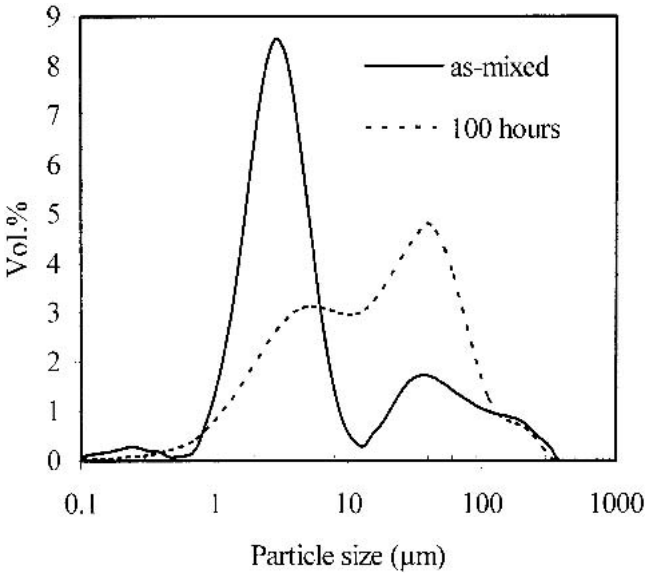

Fig. 5 Graph showing particle size distribution plots obtained from laser diffractometer measurements on powder samples in the following conditions, as shown by the legend: as-mixed Ni(Cr) and C powders and Ni(Cr) and C powders following milling for 100 h.

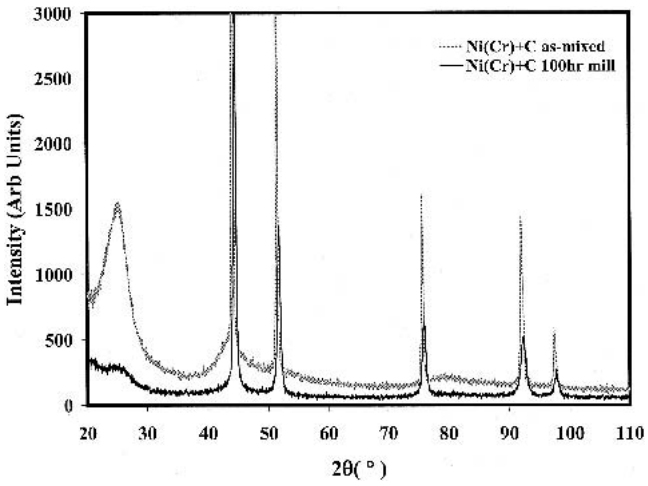

Fig. 6 The XRD patterns obtained from Ni(Cr) + C powder samples in the as-mixed condition and following 100 h of milling, as shown by the legend. High-intensity peaks corresponding to crystalline fcc Ni are present in both plots. There is a broad peak at 2θ values of ~25° from carbon in the as-mixed sample, but only a low-intensity amorphous halo in the milled sample.

Ti, Ni, and C, and thin, intersplat, oxygen-rich bands, which are presumably oxide. Figure 11(b) reveals second-phase particles in the size range 50 to 200 nm, within an individual splat, which EDX analysis showed to be rich in Ti and C and is therefore presumably nanoscale TiC grains. The XRD pattern from the as-deposited coating, shown in Fig. 12, has major peaks that can be identified as belonging to a Ni-rich solid solution phase and TiC. The diffraction peaks from TiC therefore confirm its presence within the deposit and suggest that the SHS reaction, to produce the carbide phase, occurred in individual powder particles during spraying. The Ni-based peaks were found to be

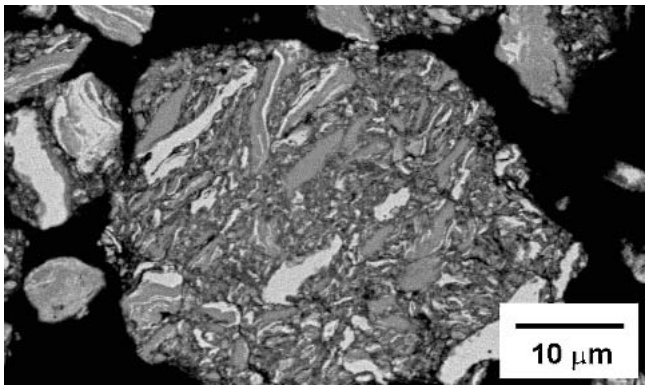

Fig. 7 A BSE image of a section through a powder particle following the milling together for 100 h of premilled Ni(Cr)-Ti and Ni(Cr)-C powders. The fine-scale layered microstructure comprises Ti-rich regions (bright) and Ni-rich regions (dark).

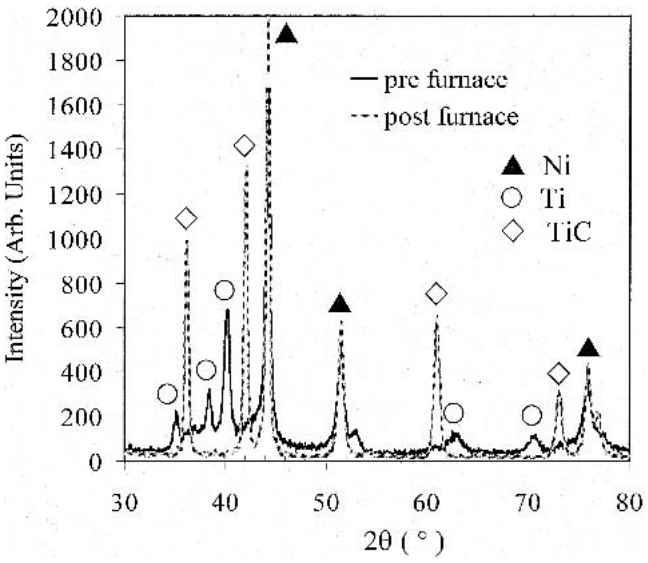

Fig. 8 The XRD patterns obtained from Ni(Cr)-Ti-C powder samples in the following conditions, as shown by the legend: after 100 h of milling of Ni(Cr)-Ti and Ni(Cr)-C powders (prefurnace) and after 100 h of milling with a subsequent short furnace anneal at 900 °C (post furnace). Crystalline peaks for TiC are present only in the postfurnace sample.

shifted to lower 2θ values than pure Ni, indicating the occurrence of lattice expansion arising from solid solution elements. Similarly, the TiC peaks were displaced from the 2θ values expected for stoichiometric TiC. A similar peak shift was also observed in TiC with micrometer-sized grains produced by bulk SHS reaction (Ref 4, 5) and is generally attributed to the formation of TiC with a substoichiometric carbon content (Ref 16). The high intensity of the TiC peaks suggests an appreciable volume fraction in the as-sprayed coating. It is notable that peaks from elemental Ti are not observed in the XRD pattern of Fig. 12, suggesting that if any unreacted Ti was present in the coating, the quantity was no greater that ~2%. However, in Fig. 12 small peaks arising from the presence of NiTi, TiO_2, and $NiTiO_3$ can be observed, which suggests that the quantities of these phases present after spraying was ~5%.

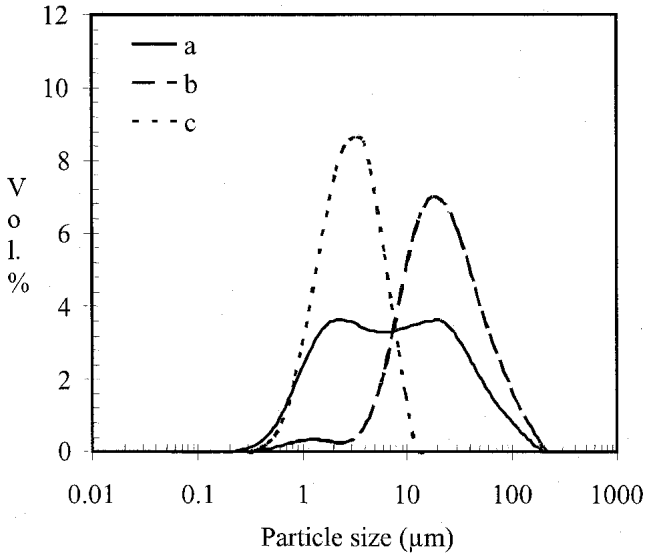

Fig. 9 Graph showing particle size distribution plots obtained from laser diffractometer measurements on milled Ni(Cr)-Ti-C powder samples. (a) As-milled, prior to classification. (b) The smaller size-fraction following classification. (c) The larger size-fraction after classification

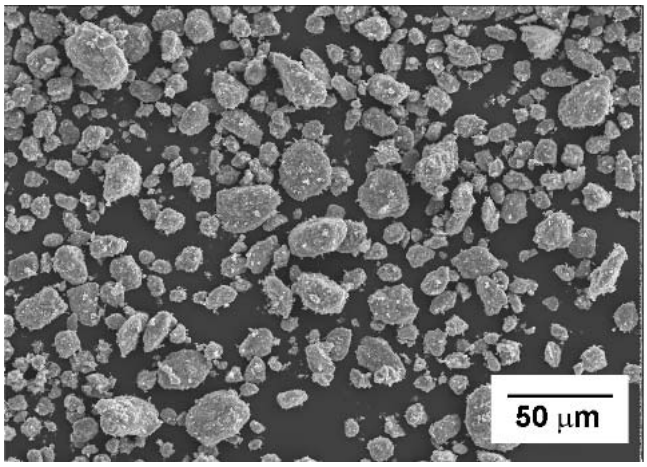

Fig. 10 Secondary electron image of the external powder morphology of the larger size-fraction Ni(Cr)-Ti-C powder after classification, which was used in the HVOF spraying experiments

4. Discussion

It is important to consider two aspects of the results, namely, the microstructure and phases formed in the powder by milling/MA and the constitution of the deposits produced by HVOF spraying.

In a series of preliminary experiments, referred to in an earlier section, attempts were made to produce a metastable powder (in which TiC did not form) by milling Ni(Cr), Ti, and C powders in a single stage. These experiments proved to be unsuccessful because TiC was produced by an explosive SHS reaction once the powder was removed from the inert atmosphere of the mill and exposed to air. This observation is consistent with work

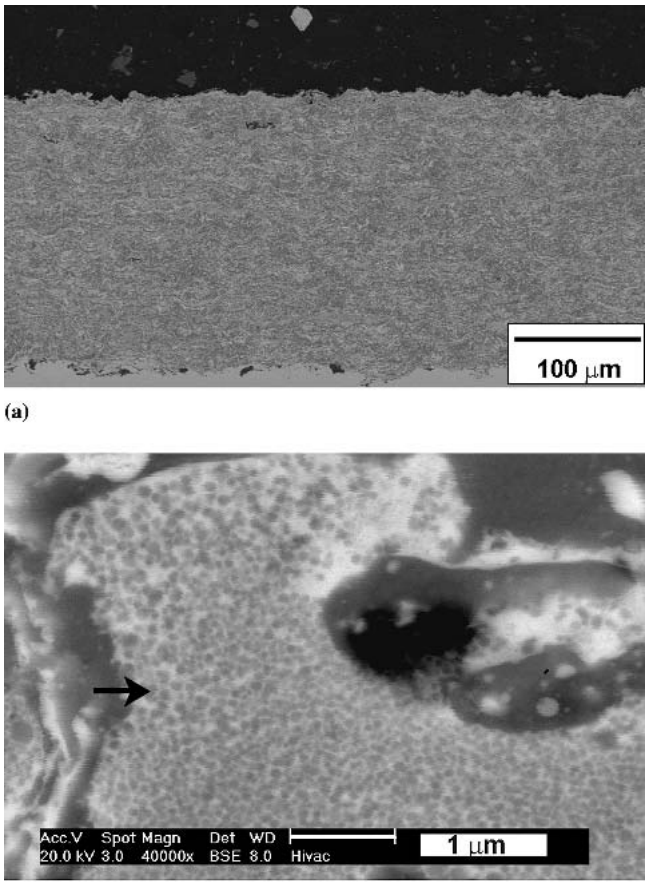

Fig. 11 (a) Low-magnification BSE image of a cross section through an HVOF-sprayed coating showing a characteristic layered morphology with little porosity in the coating. (b) A high-magnification BSE image of a region from (a) showing gray-contrast, nanoscale TiC grains (arrowed), which are embedded in a light contrast metallic matrix, as part of an individual splat. Regions of dark contrast oxide are also evident.

reported previously by various authors (Ref 8, 17-21) who examined the synthesis of TiC and Ni(Cr)-TiC composites by MA of the elemental powders. The product of milling/MA was found to depend on the milling intensity, milling time, and the atmosphere within the milling chamber. Milling in an inert atmosphere at high intensity (Ref 17-19, 21), or in air at lower intensity (Ref 20), led to the formation of TiC after a critical milling time by a highly exothermic SHS reaction within the mill. However, lower-intensity milling in an inert atmosphere led to the formation of a metastable product (Ref 8, 20), which, in the case of Wu et al. (Ref 8), reacted explosively on removal from the chamber, as was also found in the current study. Calos et al. (Ref 17) and Ye and Quan (Ref 19) have explained the mechanically initiated SHS reaction forming TiC in terms of the attainment of a critical level of lattice strain within the Ti, which opens up high-diffusivity paths for the C atoms. This allows a critical C level to build up quickly within Ti particles, sufficient to initiate the exothermic reaction, which then self-propagates as a result of the large negative enthalpy of formation of TiC. If, however, the milling intensity and time is insufficient to generate the necessary defect structure for SHS to initiate, as is the case in this

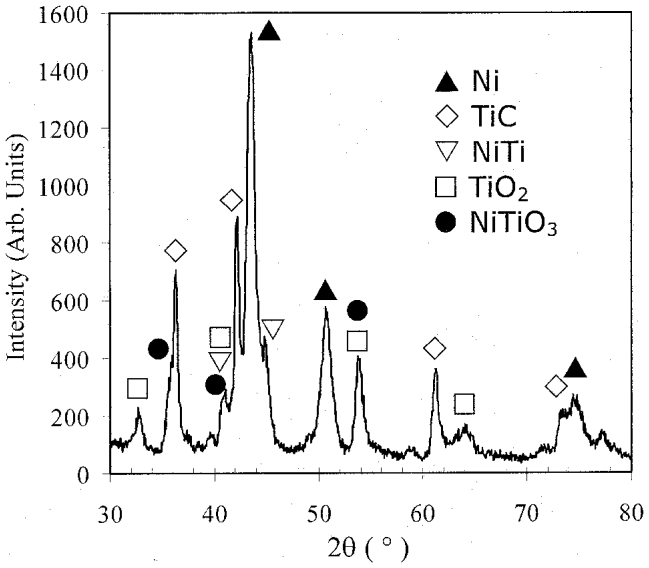

Fig. 12 The XRD pattern obtained from the as-sprayed coating shown in Fig. 11. The main peaks correspond to an fcc Ni solid solution and TiC, with smaller peaks corresponding to NiTi, TiO_2, and $NiTiO_3$.

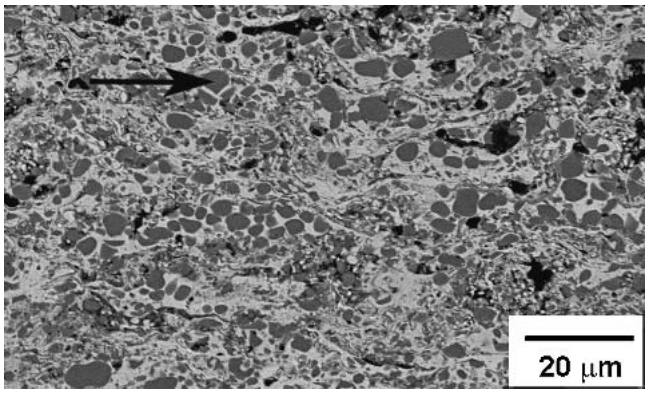

Fig. 13 A low-magnification BSE image of a cross section through an HVOF-sprayed coating deposited with powder produced using a conventional SHS route. Micron-sized, TiC particles of gray contrast (arrowed) are embedded in a light-contrast Ni-rich matrix, with intersplat oxide layers (dark) (Ref 5).

study and also in the work of Wu et al. (Ref 8), then the explosive combustion and formation of TiC on exposure to air could well be initiated by the highly exothermic reaction involving oxidation of the clean Ti surfaces generated by inert atmosphere milling. Furthermore, milling will have generated large surface area-to-volume ratios in both Ti and C powders, which enhances reactivity.

With regard to the main results involving the production of metastable Ni(Cr)-Ti-C powder (which did not react on removal from the mill and exposure to air), the critical step was found to be premilling Ni(Cr) and Ti and premilling Ni(Cr) and C prior to combining them for a further milling period. This approach presumably reduced the chemical activity of the C by dissolving a proportion of it in the Ni(Cr) phase and also caused free carbon to be embedded within the nonreactive Ni(Cr) phase, as seen in Fig. 4. Similarly, the premilling of Ni(Cr) and Ti powders forms a layered structure (Fig. 1) prior to introduction of the Ni(Cr)-C powder into the mill. Thus, although the final powder microstructure (Fig. 7) contains Ti, Ni(Cr), and C all embedded in the same particle, there is a decreased possibility of fresh Ti surfaces being in contact with free C and simultaneously exposed to air on removal from the mill. Consequently, the possibility of Ti oxidation initiating the SHS of TiC is greatly diminished.

It is evident, however, that TiC can be produced from the metastable powder product of the current study both during furnace heating of the compacted powder (Fig. 8) and in the HVOF spray process (Fig. 12). Although Choi (Ref 20) and Huang et al. (Ref 21) have been able to form TiC from a metastable powder compact by furnace heating, the current study appears to be the first to report TiC formation as a result of thermal spraying. However, it is difficult to determine precisely at what point in the spray process the TiC particles formed and the mechanism involved. TiC could have been produced during powder heating in the HVOF gun, either in the solid state or during melting of the Ni-rich phase, or it could have nucleated and solidified from the Ni-rich molten phase during rapid cooling of the splats. Irrespective of the precise mechanism of formation, it is significant that the TiC particles are found in the coating on a very fine scale (Fig. 11) and are on the order of 50 to 200 nm in size. This is significantly smaller than the 0.5 to 1 μm size reported for the particles of furnace-sintered material (Ref 20) and so could suggest nucleation during rapid solidification as being more likely.

Finally, it is of interest to compare the present reactively sprayed deposits with Ni(Cr)-TiC cermet coatings produced from conventional SHS feedstock powder (Ref 1-5). While the microstructure and properties of these latter materials are attractive, a difficulty lies in the grinding process for powder production, in that the yields of powder within a sprayable range, typically 10 to 45 μm, are low (on the order of 25%) (Ref 5). This is because TiC-based cermets are extremely hard materials requiring high-intensity grinding processes to crush them, such as a ring-and-puck mill, and the process results in a high proportion of fines, which are, to a large extent, individual TiC particles. There is clearly considerable advantage in producing powder particles that contain the elements required to produce TiC in a Ni(Cr) matrix by a less intensive route that, when sprayed, then reacts to generate the hard TiC component, as in the current study.

By way of comparison, Fig. 13 shows the microstructure of a coating, of nominal composition 35wt.%Ni(Cr)-65wt.%TiC, produced from powder that was generated using a conventional SHS method (Ref 5), that is, the elemental Ni(Cr), Ti, and C powders were mixed to form a compact and were ignited to initiate the SHS reaction, the product of which was then crushed, ground, and classified into powder with particles in the range 8 to 38 μm. In this coating, the TiC particles ~5 μm in size are uniformly dispersed in the Ni-rich matrix. Comparison of this microstructure (Fig. 13) with that of the coating shown in Fig. 11 reveals a major difference, in that the size of the TiC grains is significantly decreased in the reactively sprayed material. However, the overall proportion of TiC in the reactively sprayed coating was lower than that expected from the nominal powder composition. A number of reasons can be proposed to account for this. The first is the initial milling of the Ni(Cr) and C during step 2. Equal weights (50 g) of Ni(Cr) and C were introduced

into the milling chamber. However, the volume of each constituent was considerably different, calculated to be three volumes of C to one of Ni(Cr). Therefore, there was insufficient volume of Ni(Cr) to accommodate high levels of C, and as a result, even after 100 h of milling, significant amounts of free C remained. Taking this material on to step 3 may have resulted in some of this free C being mechanically alloyed further within the Ni(Cr)-Ti particles. However, only a limited amount would have been incorporated. This inability to fully accommodate all the C can be seen in the particle size analysis (Fig. 9), in which the left-hand side of the bimodal distribution is probably free C. Obviously, after air classification this C was removed and, thus, was not available to form TiC. Hence, the overall proportion of TiC in the coating was smaller than the initial 50 wt.% target. Even if the powder had been sprayed with a particle-size distribution at the preclassification stage, exposure to the high temperature and oxygen within the combustion flame would have resulted in oxidation and the loss of the free C. A further consequence of the stoichiometric imbalance of Ti to C in the classified MA powder was the formation of small quantities of TiO_2, $NiTiO_3$, and NiTi during spraying (Fig. 12). An important final point is that this reactive spraying technique produced nanoscale TiC, and this may have important consequences for the physical and mechanical properties of the coatings, which requires further investigation.

5. Conclusions

1. A planar-type mill (Uni-Ball II, , Australian Scientific Instruments) was successfully used to produce a range of mechanically alloyed powders.
2. The milling together of Ni(Cr) + Ti + C powders produced an unstable product, which spontaneously underwent SHS reaction on exposure to air following milling.
3. Utilizing a three-step process whereby Ni(Cr) + Ti, Ni(Cr) + C powders were milled separately for 100 h, and then combined together and milled for a further 100 h produced a metastable powder that was capable of undergoing a reaction to form TiC during either furnace heating or HVOF spraying.
4. When the metastable powder was HVOF-sprayed to give a coating ~250 μm thick, it was found to comprise TiC, Ni-rich solid solution, and smaller quantities of NiTi and oxides. The TiC grains were found to be typically 50 to 200 nm in size.

Acknowledgment

The authors acknowledge financial support from the Engineering and Physical Sciences Research Council (EPSRC) through the award of a research grant (GR/M03474). They are also grateful to London & Scandinavian Metallurgical Co. Ltd. for supplying materials and for the use of the air-classification facility. Thanks are also due to Prof. T. Hyde for the provision of laboratory facilities.

References

1. J.M. de Paco, J. Nutting, J.M. Guilemany, F.J. Sanchez, J.R. Miguel, and P. Smith, Structure-Property Relationships of TiC-Ni + Ti and (Ti,W)C-Ni Powders Manufactured by the SHS Process, and the Resultant HVOF-Sprayed Coatings, *Thermal Spray: A United Forum for Scientific and Technological Advances,* C.C. Berndt, Ed. Sept 15-18, 1997 (Indianapolis, IN), ASM International, 1997, p 935-942
2. M. Vasianen, P. Vuoristo, T. Mantyla, J. Maunu, P. Lintunen, and P. Lintula, Microstructure and Properties of TiC-CrNiMo SHS Spray Powder and Thermally Sprayed Coatings, *Thermal Spray: Surface Engineering via Applied Research,* C.C. Berndt, Ed., May 8-11, 2000 (Montréal, Québec, Canada), ASM International, 2000, p 429-434
3. J.M. Guilemany, J.M. de Paco, J.R. Miguel, F.J. Sanchez, and P. Smith, Corrosion Resistance HVOF Coatings Based Upon TiC + NiTi and (Ti,W)C + Ni, *Thermal Spray: Meeting the Challenges of the 21st Century,* C. Coddet, Ed., May 25-29, 1998 (Nice, France), ASM International, 1998, p 57-61
4. M. Jones, A.J. Horlock, P.H. Shipway, D.G. McCartney, and J.V. Wood, Microstructure and Abrasive Wear Behaviour of FeCr-TiC Coatings Deposited by HVOF Spraying of SHS Powders, *Wear,* Vol 249, 2001, p 246-253
5. M.T. Blatchford, A.J. Horlock, P.H. Shipway, D.G. McCartney, and J.V. Wood, Production and Characterisation of HVOF Sprayed Ni(Cr)-TiC Coatings Using SHS Powder Feedstock, *Thermal Spray: Surface Engineering via Applied Research,* C.C. Berndt, Ed., May 8-11, 2000 (Montréal, Québec, Canada), ASM International, 2000, p 515-521
6. J.J. Moore and H.J. Feng, Combustion Synthesis of Advanced Materials, *Prog. Mater. Sci.,* Vol 39, 1995, p 243-273
7. C. Bartuli, R.W. Smith, and E. Shtessel, SHS Powders for Thermal Spray Applications, *Ceram. Int.,* Vol 23, 1997, p 61-68
8. N.Q. Wu, G.-X. Wang, J.M. Wu, Z.Z. Li, and M.Y. Yuan, Investigation of TiC Formation During Ball-milling of Elemental Titanium and Carbon, *Int. J. Refract. Met. Hard Mater.,* Vol 15, 1997, p 289-293
9. Fr.-W. Bach, Z. Babiak, T. Duda, T. Rothardt, and G. Tegeder, Impact of Self-Propagating High Temperature Synthesis of Spraying Materials on Coatings Based on Aluminium and Metal-Oxides, *Thermal Spray: New Surfaces for a New Millennium,* C.C. Berndt, Ed., May 28-30, 2001 (Singapore), ASM International, 2001, p 497-502
10. S. Dallaire and B. Champagne, Plasma Spray Synthesis of TiB_2-Fe Coatings, *Thin Solid Films,* Vol 118, 1984, p 477-483
11. J.S. Benjamin, Mechanical Alloying, *Sci. Am.,* Vol 234 (No. 5), 1976, p 40-48
12. L. Lu and M.O. Lai, *Mechanical Alloying,* Kluwer Academic Publishers, Boston 1998
13. A. Calka and A.P. Radlinski, Universal High Performance Ball-Milling Device and Its Application for Mechanical Alloying, *Mater. Sci. Eng., A,* Vol 143, 1991, p 1350-1353
14. A. Calka and J.I. Nikolov, The Dynamics of Magneto-Ball Milling and Its Effect on Phase Transformations During Mechanical Alloying, *Mater. Sci. Forum,* Vol 179-181, 1995, p 333-338
15. L. Pawlowski, *The Science and Engineering of Thermal Spray Coatings,* John Wiley & Sons, Chichester, U.K., 1995
16. H.E. Exner, Physical and Chemical Nature of Cemented Carbides, *Int. Met. Rev.,* Vol 4, 1979, p 149-173
17. N.J. Calos, J.S. Forrester, and G.B. Schaffer, The Mechanisms of Combustion and Continuous Reactions During Mechanical Alloying, *J. Solid State Chem.,* Vol 158, 2001, p 268-278
18. Z. Xinkun, Z. Kunyu, C. Baochang, L. Qiushi, Z. Xiuqin, C. Tieli, and S. Yunsheng, Synthesis of Nanocrystalline TiC Powder by Mechnical Alloying, *Mater. Sci. Eng., C,* Vol 16, 2001, p 103-105
19. L.L. Ye and M.X. Quan, Synthesis of Nanocrystalline TiC Powders by Mechanical Alloying, *Nanostruct. Mater.,* Vol 5, 1995, p 25-31
20. C.-J. Choi, Preparation of Ultrafine TiC-Ni Cermet Powders by Mechanical Alloying, *J. Mater. Process. Technol.,* Vol 104, 2000, p 127-132
21. J.Y. Huang, L.L. Ye, Y.K. Wu, and H.Q. Ye, Microstructure Investigations of Explosive TiNi (or Ni)/TiC-Composite-Formation Reaction During Mechanical Alloying, *Acta Mater.,* Vol 44, 1996, p 1781-1792